IV International Conference on Computational Methods for Coupled Problems in Science and Engineering
COUPLED PROBLEMS 2011
M. Papadrakakis, E. Oñate and B. Schrefler (Eds)

A NEW NUMERICAL SCHEME FOR A LINEAR FLUID–STRUCTURE INTERACTION PROBLEM

MARÍA GONZÁLEZ* AND VIRGINIA SELGAS*

*Departamento de Matemáticas
Facultad de Informática, Universidad de A Coruña
Campus de Elviña, 15071 A Coruña, Spain
e-mails: mgtaboad@udc.es and vselgas@udc.es

Key words: Fluid-structure interaction, incompressible fluid, linear elasticity, finite element method

Abstract. We consider a linear fluid–structure interaction problem consisting of the time-dependent Stokes equations coupled with those of linear elastodynamics. We assume that the fluid and the solid interact through a fixed interface. Then, we reformulate the problem following the ideas of [6], and propose a new monolithic method in terms of the velocity (both in the fluid and the solid) and the fluid pressure. We discretize the problem using the implicit Euler method for the time variable, piecewise linear elements in the solid and the mini-element in the fluid domain. Displacements in the structure can be recovered by means of a quadrature formula. Our numerical results confirm the robustness and good convergence properties of the proposed scheme. Moreover, our approach is easy to implement as compared with other methods available in the literature.

1 INTRODUCTION

We consider a time-dependent system modeling the interaction between a Stokes fluid and an elastic structure in two or three dimensional bounded domains, and assume that the interface between the fluid and the solid is fixed. This model was studied in [2, 3] and can be used when the solid undergoes only infinitesimal elastic displacements but its velocity is large enough so that the fluid and the structure remain fully coupled; see [2] for more details.

In [2], a divergence-free weak formulation of this problem, that does not involve the fluid pressure field, was introduced and analyzed. The existence and uniqueness of a weak solution was proved and, under some additional assumptions on the data, strong energy estimates and the existence of a L^2-integrable pressure field were derived. Semidiscrete finite element approximations were defined and studied in [3]. The existence of finite element solutions is proved there using an auxiliary discretely divergence-free formulation

and a discrete inf-sup condition, that allows to establish the existence of a finite element pressure. Strong a priori estimates for the finite element solutions and semidiscrete error estimates were also derived in [3]. Previous work concerning this model include, besides [2, 3], eigenmode analysis [7], homogenization [1], the one-dimensional case [4] and a numerical algorithm [5].

In this work, we reformulate the problem following the ideas of [6], and propose a new fully discrete scheme in terms of the velocity (both in the fluid and the solid) and the fluid pressure. We then discretize the problem using the implicit Euler method for the time variable, the mini-element for the Stokes problem and piecewise linear elements in the solid domain. As we will see, displacements in the structure can be recovered using a quadrature formula. We remark that this new approach is easy to implement and the numerical experiments carried out confirm its robustness and good convergence properties.

2 MODEL PROBLEM

We assume that the fluid and the solid occupy two adjacent Lipschitz domains, $\Omega_F \subset \mathbb{R}^d$ and $\Omega_S \subset \mathbb{R}^d$, respectively, where $d = 2$ or 3 is the space dimension. We let $\Sigma := \partial\Omega_F \cap \partial\Omega_S$ denote the interface between the fluid and the solid, and let $\Gamma_F := \partial\Omega_F \setminus \Sigma$ and $\Gamma_S := \partial\Omega_S \setminus \Sigma$ denote, respectively, the parts of the fluid and solid boundaries excluding the interface Σ; we assume that $\mathrm{meas}(\Gamma_F \cup \Gamma_S) \neq 0$. Finally, we denote by Ω the entire fluid–solid region, that is, $\Omega := \Omega_F \cup \Sigma \cup \Omega_S$. In the figure below, we represent from left to right the situations where $\Gamma_F = \emptyset$, $\Gamma_S \neq \emptyset$ or $\Gamma_F \neq \emptyset \neq \Gamma_S$.

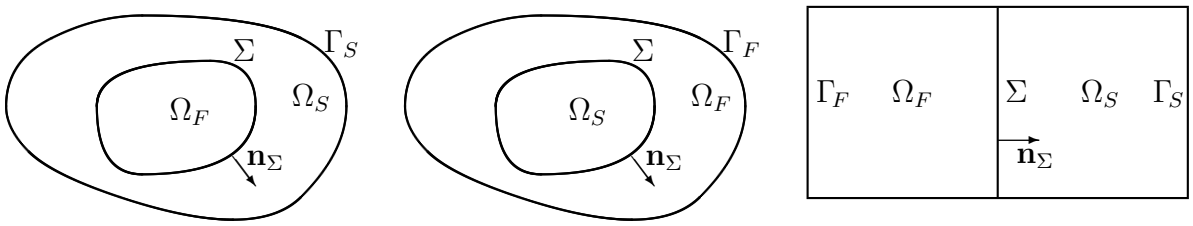

Figure 1: Domain of the problem. Cases $\Gamma_F = \emptyset$, $\Gamma_S \neq \emptyset$ and $\Gamma_F \neq \emptyset \neq \Gamma_S$.

Given $T > 0$, we consider a time-dependent Stokes fluid in Ω_F:

$$\left\{\begin{array}{rcll} \rho_F\,\partial_t \mathbf{v}_F - \mathbf{div}(\boldsymbol{\sigma}_F) &=& \mathbf{f}_F & \text{in } (0,T)\times\Omega_F, \\ \boldsymbol{\sigma}_F &=& -p\,I + 2\,\nu\,\boldsymbol{\varepsilon}(\mathbf{v}_F) & \text{in } (0,T)\times\Omega_F, \\ \mathrm{div}(\mathbf{v}_F) &=& 0 & \text{in } (0,T)\times\Omega_F, \\ \mathbf{v}_F &=& \mathbf{0} & \text{on } (0,T)\times\Gamma_F, \\ \mathbf{v}_F(0) &=& \mathbf{v}_F^0 & \text{in } \Omega_F, \end{array}\right. \tag{1}$$

where $\mathbf{v}_F$ denotes the fluid velocity, $\boldsymbol{\sigma}_F$ the fluid stress tensor, $\mathbf{f}_F$ the given fluid body force, p the fluid pressure, ρ_F the constant fluid density, ν the kinematic viscosity and $\mathbf{v}_F^0$ is the given initial fluid velocity. We recall that $\boldsymbol{\varepsilon}(\mathbf{v}) := \frac{1}{2}\left(\nabla \mathbf{v} + (\nabla \mathbf{v})^{\mathtt{t}}\right)$ denotes the strain tensor of small deformations.

In the solid region Ω_S, we consider the equations of linear elasticity:

$$\left\{\begin{array}{rcll} \rho_S\, \partial_{tt}\mathbf{u}_S \,-\, \mathbf{div}(\boldsymbol{\sigma}_S) &=& \mathbf{f}_S & \text{in } (0,T)\times\Omega_S, \\ \boldsymbol{\sigma}_S &=& \lambda\, \mathrm{div}(\mathbf{u}_S)\, I + 2\,\mu\, \boldsymbol{\varepsilon}(\mathbf{u}_S) & \text{in } (0,T)\times\Omega_S, \\ \mathbf{u}_S &=& \mathbf{0} & \text{on } (0,T)\times\Gamma_S, \\ \mathbf{u}_S(0) &=& \mathbf{u}_S^0 & \text{in } \Omega_S, \\ \partial_t \mathbf{u}_S(0) &=& \mathbf{v}_S^0 & \text{in } \Omega_S, \end{array}\right. \tag{2}$$

where $\mathbf{u}_S$ denotes the displacement of the solid, $\boldsymbol{\sigma}_S$ the Cauchy stress tensor, $\mathbf{f}_S$ the given loading force, ρ_S the constant solid density and λ and μ are the Lamé constants. The given initial data, $\mathbf{u}_S^0$ and $\mathbf{v}_S^0$, represent, respectively, the initial displacement and the initial structural velocity.

We assume further that the velocity and the normal stresses are continuous across the interface Σ:

$$\mathbf{v}_F = \partial_t \mathbf{u}_S \quad \text{and} \quad \boldsymbol{\sigma}_F \mathbf{n}_\Sigma = \boldsymbol{\sigma}_S \mathbf{n}_\Sigma \qquad \text{on } (0,T)\times\Sigma, \tag{3}$$

where $\mathbf{n}_\Sigma$ is the unit normal vector along Σ pointing to Ω_S; see Figure 1.

3 A WEAK FORMULATION

In order to propose a new numerical scheme to solve problem (1)–(3), we first derive a weak formulation for the problem in terms of the the fluid velocity $\mathbf{v}_F$, the structural velocity $\mathbf{v}_S := \partial_t \mathbf{u}_S$, and the pressure field p. In what follows, given a scalar or vector field $\xi \equiv \xi(t,\mathbf{x})$, we denote $\xi(t) := \xi(t,\cdot)$.

Multiplying the first equation of (1) by a test function $\mathbf{w}\colon \Omega_F \to \mathbb{R}^d$ such that $\mathbf{w} = \mathbf{0}$ on Γ_F, and integrating by parts, we obtain:

$$\rho_F \frac{d}{dt}\int_{\Omega_F} \mathbf{v}_F \cdot \mathbf{w} \,+\, \int_{\Omega_F} \boldsymbol{\sigma}_F : \boldsymbol{\varepsilon}(\mathbf{w}) \,-\, \int_\Sigma \boldsymbol{\sigma}_F \mathbf{n}_\Sigma \cdot \mathbf{w} \,=\, \int_{\Omega_F} \mathbf{f}_F \cdot \mathbf{w}\,. \tag{4}$$

Then, using the definition of $\boldsymbol{\sigma}_F$, we can write

$$\rho_F \frac{d}{dt}\int_{\Omega_F} \mathbf{v}_F\cdot\mathbf{w} - \int_{\Omega_F} p\,\mathrm{div}(\mathbf{w}) + 2\,\nu \int_{\Omega_F} \boldsymbol{\varepsilon}(\mathbf{v}_F) : \boldsymbol{\varepsilon}(\mathbf{w}) - \int_\Sigma \boldsymbol{\sigma}_F \mathbf{n}_\Sigma \cdot \mathbf{w} \,=\, \int_{\Omega_F} \mathbf{f}_F \cdot \mathbf{w}\,. \tag{5}$$

On the other hand, the weak formulation of the third equation in (1) is

$$\int_{\Omega_F} q\,\mathrm{div}(\mathbf{v}_F) = 0 \qquad \forall\, q \in L^2(\Omega_F)\,. \tag{6}$$

In the solid region Ω_S, we rewrite the equations of linear elasticity in terms of the structural velocity, $\mathbf{v}_S = \partial_t \mathbf{u}_S$, and the stress tensor, $\boldsymbol{\sigma}_S$:

$$\left\{\begin{array}{rcll} \rho_S\,\partial_t \mathbf{v}_S \,-\, \mathbf{div}(\boldsymbol{\sigma}_S) &=& \mathbf{f}_S & \text{in } (0,T)\times\Omega_S, \\ \partial_t\,\boldsymbol{\sigma}_S &=& \lambda\,\mathrm{div}(\mathbf{v}_S)\,I + 2\,\mu\,\boldsymbol{\varepsilon}(\mathbf{v}_S) & \text{in } (0,T)\times\Omega_S, \\ \mathbf{v}_S &=& \mathbf{0} & \text{on } (0,T)\times\Gamma_S, \\ \mathbf{v}_S(0) &=& \mathbf{v}_S^0 & \text{in } \Omega_S, \\ \boldsymbol{\sigma}_S(0) &=& \boldsymbol{\sigma}_S^0 & \text{in } \Omega_S, \end{array}\right. \tag{7}$$

where $\boldsymbol{\sigma}_S^0 := \lambda\,\mathrm{div}(\mathbf{u}_S^0)\,I + 2\,\mu\,\boldsymbol{\varepsilon}(\mathbf{u}_S^0)$. We remark that the displacement of the solid $\mathbf{u}_S$ can then be recovered as

$$\mathbf{u}_S(t) = \mathbf{u}_S^0 + \int_0^t \mathbf{v}_S(s)\,ds\,, \tag{8}$$

and that the first coupling condition in (3) can be written as

$$\mathbf{v}_F = \mathbf{v}_S \qquad \text{on } (0,T)\times\Sigma\,. \tag{9}$$

Multiplying the first equation of (7) by a test function $\mathbf{w}\colon \Omega_S \to \mathbb{R}^d$ such that $\mathbf{w} = \mathbf{0}$ on Γ_S and integrating by parts, we obtain:

$$\rho_S\,\frac{d}{dt}\int_{\Omega_S} \mathbf{v}_S\cdot\mathbf{w} \,+\, \int_{\Omega_S} \boldsymbol{\sigma}_S : \boldsymbol{\varepsilon}(\mathbf{w}) \,+\, \int_{\Sigma} \boldsymbol{\sigma}_S\mathbf{n}_\Sigma\cdot\mathbf{w} \,=\, \int_{\Omega_S} \mathbf{f}_S\cdot\mathbf{w}\,. \tag{10}$$

Then, multiplying the second equation of (7) by a test function $\boldsymbol{\tau}$ defined in Ω_S, and integrating in Ω_S, we get

$$\frac{d}{dt}\int_{\Omega_S} \boldsymbol{\sigma}_S : \boldsymbol{\tau} \,=\, \lambda\int_{\Omega_S} \mathrm{div}(\mathbf{v}_S)\mathrm{tr}(\boldsymbol{\tau}) \,+\, 2\,\mu\int_{\Omega_S} \boldsymbol{\varepsilon}(\mathbf{v}_S) : \boldsymbol{\tau}\,. \tag{11}$$

Taking into account the coupling condition (9), it is reasonable to look for a global unknown $\mathbf{v}(t) \in \mathbf{H}^1_0(\Omega)$ defined by

$$\mathbf{v} := \left\{\begin{array}{ll} \mathbf{v}_F & \text{in } (0,T)\times\Omega_F\,, \\ \mathbf{v}_S & \text{in } (0,T)\times\Omega_S\,, \end{array}\right. \tag{12}$$

and consider global test functions $\mathbf{w} \in \mathbf{H}^1_0(\Omega)$. We also define

$$\rho := \left\{\begin{array}{ll} \rho_F & \text{in } \Omega_F\,, \\ \rho_S & \text{in } \Omega_S\,, \end{array}\right. \qquad \mathbf{f} := \left\{\begin{array}{ll} \mathbf{f}_F & \text{in } (0,T)\times\Omega_F\,, \\ \mathbf{f}_S & \text{in } (0,T)\times\Omega_S\,, \end{array}\right. \tag{13}$$

and introduce a global version of the initial data,

$$\mathbf{v}^0 := \left\{\begin{array}{ll} \mathbf{v}_F^0 & \text{in } \Omega_F\,, \\ \mathbf{v}_S^0 & \text{in } \Omega_S\,. \end{array}\right. \tag{14}$$

Then, summing up equations (5) and (10), and using the second coupling condition in (3), we obtain

$$\frac{d}{dt}\int_\Omega \rho\,\mathbf{v}\cdot\mathbf{w} \,+\, 2\,\nu\int_{\Omega_F}\boldsymbol{\varepsilon}(\mathbf{v}_F):\boldsymbol{\varepsilon}(\mathbf{w}) \,+\, \int_{\Omega_S}\boldsymbol{\sigma}_S:\boldsymbol{\varepsilon}(\mathbf{w}) \,-\, \int_{\Omega_F} p\,\mathrm{div}(\mathbf{w}) = \int_\Omega \mathbf{f}\cdot\mathbf{w}\,, \quad (15)$$

for any $\mathbf{w}\in\mathbf{H}^1_0(\Omega)$.

Therefore, given $\mathbf{v}^0$ and $\boldsymbol{\sigma}_S^0$, a weak formulation for the fluid–structure interaction problem (1)–(3) reads:
For each $t\in(0,T]$, find $\mathbf{v}(t)\in\mathbf{H}^1_0(\Omega)$, $p(t)\in L^2(\Omega_F)$ and $\boldsymbol{\sigma}_S(t)\in\mathbf{L}^2_{\mathtt{sym}}(\Omega_S)$ such that

$$\left\{\begin{array}{l} \dfrac{d}{dt}\displaystyle\int_\Omega \rho\,\mathbf{v}\cdot\mathbf{w} \,+\, 2\,\nu\int_{\Omega_F}\boldsymbol{\varepsilon}(\mathbf{v}_F):\boldsymbol{\varepsilon}(\mathbf{w}) \,+\, \int_{\Omega_S}\boldsymbol{\sigma}_S:\boldsymbol{\varepsilon}(\mathbf{w}) \,-\, \int_{\Omega_F} p\,\mathrm{div}(\mathbf{w}) = \int_\Omega \mathbf{f}\cdot\mathbf{w}\,, \\ \dfrac{d}{dt}\displaystyle\int_{\Omega_S}\boldsymbol{\sigma}_S:\boldsymbol{\tau} = \lambda\int_{\Omega_S}\mathrm{div}(\mathbf{v}_S)\mathrm{tr}(\boldsymbol{\tau}) \,+\, 2\,\mu\int_{\Omega_S}\boldsymbol{\varepsilon}(\mathbf{v}_S):\boldsymbol{\tau}\,, \\ \displaystyle\int_{\Omega_F} q\,\mathrm{div}(\mathbf{v}_F) = 0\,, \\ \mathbf{v}(0)=\mathbf{v}^0 \quad \text{in } \Omega, \qquad \boldsymbol{\sigma}_S(0)=\boldsymbol{\sigma}_S^0 \quad \text{in } \Omega_S, \end{array}\right. \quad (16)$$

for all $\mathbf{w}\in\mathbf{H}^1_0(\Omega)$, $\boldsymbol{\tau}\in\mathbf{L}^2_{\mathtt{sym}}(\Omega_S)$ and $q\in L^2(\Omega_F)$, where

$$\mathbf{L}^2_{\mathtt{sym}}(\Omega_S) := \left\{\boldsymbol{\sigma}\in[L^2(\Omega_S)]^{d\times d} \,:\, \boldsymbol{\sigma}^{\mathtt{t}}=\boldsymbol{\sigma} \text{ in } \Omega_S\right\}. \quad (17)$$

4 FULLY DISCRETE SCHEME

4.1 Time discretization

Let N be a given nonnegative integer. We first consider a uniform partition of $[0,T]$, $\{t_n\}_{n=0}^N$, and denote $\Delta t := T/N$. For each time step t_n, $n=1,2,\ldots$, we approximate

$$\frac{d}{dt}\mathbf{v}(t_n) \,\approx\, \frac{\mathbf{v}(t_n)-\mathbf{v}(t_{n-1})}{\Delta t} \qquad \text{and} \qquad \frac{d}{dt}\boldsymbol{\sigma}_S(t_n) \,\approx\, \frac{\boldsymbol{\sigma}_S(t_n)-\boldsymbol{\sigma}_S(t_{n-1})}{\Delta t}\,, \quad (18)$$

and, for any scalar or vector field $\xi=\xi(t,\mathbf{x})$, we denote $\xi^n\approx\xi(t_n)$.

Then, given $\mathbf{v}^0$ and $\boldsymbol{\sigma}_S^0$, for $n=1,2,\ldots$, we solve for $\mathbf{v}^n\in\mathbf{H}^1_0(\Omega)$, $p^n\in L^2(\Omega_F)$ and $\boldsymbol{\sigma}_S^n\in\mathbf{L}^2_{\mathtt{sym}}(\Omega_S)$ such that

$$\left\{\begin{array}{l} \displaystyle\int_\Omega \rho\,\mathbf{v}^n\cdot\mathbf{w} \,+\, 2\,\nu\,\Delta t\int_{\Omega_F}\boldsymbol{\varepsilon}(\mathbf{v}_F^n):\boldsymbol{\varepsilon}(\mathbf{w}) \,+\, \Delta t\int_{\Omega_S}\boldsymbol{\sigma}_S^n:\boldsymbol{\varepsilon}(\mathbf{w}) \,-\, \Delta t\int_{\Omega_F} p^n\,\mathrm{div}(\mathbf{w}) = \\ \qquad\qquad = \Delta t\displaystyle\int_\Omega \mathbf{f}(t_n)\cdot\mathbf{w} \,+\int_\Omega \rho\,\mathbf{v}^{n-1}\cdot\mathbf{w}\,, \\ \displaystyle\int_{\Omega_S}\boldsymbol{\sigma}_S^n:\boldsymbol{\tau} = \lambda\,\Delta t\int_{\Omega_S}\mathrm{div}(\mathbf{v}_S^n)\mathrm{tr}(\boldsymbol{\tau}) \,+\, 2\,\mu\,\Delta t\int_{\Omega_S}\boldsymbol{\varepsilon}(\mathbf{v}_S^n):\boldsymbol{\tau} \,+\int_{\Omega_S}\boldsymbol{\sigma}_S^{n-1}:\boldsymbol{\tau}\,, \\ \displaystyle\int_{\Omega_F} q\,\mathrm{div}(\mathbf{v}_F^n) = 0\,, \end{array}\right. \quad (19)$$

for all $\mathbf{w} \in \mathbf{H}^1_0(\Omega)$, $\boldsymbol{\tau} \in \mathbf{L}^2_{\mathtt{sym}}(\Omega_S)$ and $q \in L^2(\Omega_F)$.

Now we remark that taking $\boldsymbol{\tau} = \boldsymbol{\varepsilon}(\mathbf{w})$ in the second equation of (19), we have that

$$\begin{aligned}\int_{\Omega_S} \boldsymbol{\sigma}_S^n : \boldsymbol{\varepsilon}(\mathbf{w}) \;&=\; \lambda\,\Delta t \int_{\Omega_S} \mathrm{div}(\mathbf{v}_S^n)\mathrm{div}(\mathbf{w}) \,+\, 2\,\mu\,\Delta t \int_{\Omega_S} \boldsymbol{\varepsilon}(\mathbf{v}_S^n) : \boldsymbol{\varepsilon}(\mathbf{w}) \\ &+\; \int_{\Omega_S} \boldsymbol{\sigma}_S^{n-1} : \boldsymbol{\varepsilon}(\mathbf{w})\end{aligned} \tag{20}$$

Then, substituting (20) in the first equation of (19), we derive the following semidiscrete in time scheme to solve problem (1)–(3):
Given $\mathbf{v}^0$ and $\boldsymbol{\sigma}_S^0$, for $n = 1, 2, \ldots$, we look for $\mathbf{v}^n \in \mathbf{H}^1_0(\Omega)$, $p^n \in L^2(\Omega_F)$ such that

$$\left\{\begin{array}{l} \displaystyle\int_\Omega \rho\,\mathbf{v}^n\cdot\mathbf{w} \,+ \int_\Omega \kappa\,\boldsymbol{\varepsilon}(\mathbf{v}^n):\boldsymbol{\varepsilon}(\mathbf{w}) \,+\, \lambda\,(\Delta t)^2 \int_{\Omega_S} \mathrm{div}(\mathbf{v}_S^n)\mathrm{div}(\mathbf{w}) - \Delta t \int_{\Omega_F} p^n\,\mathrm{div}(\mathbf{w}) \,= \\ \qquad\qquad = \,\Delta t \,\displaystyle\int_\Omega \mathbf{f}(t_n)\cdot\mathbf{w} \,+\, \int_\Omega \rho\,\mathbf{v}^{n-1}\cdot\mathbf{w} \,-\, \Delta t \int_{\Omega_S} \boldsymbol{\sigma}_S^{n-1} : \boldsymbol{\varepsilon}(\mathbf{w})\,, \\ \displaystyle\int_{\Omega_F} q\,\mathrm{div}(\mathbf{v}_F^n) = 0\,, \end{array}\right. \tag{21}$$

for all $\mathbf{w} \in \mathbf{H}^1_0(\Omega)$ and $q \in L^2(\Omega_F)$, where $\kappa := 2\,\nu\,\Delta t$ in Ω_F and $\kappa := 2\,\mu\,(\Delta t)^2$ in Ω_S. We then approximate

$$\boldsymbol{\sigma}_S(t_n) \approx \boldsymbol{\sigma}_S^n := \boldsymbol{\sigma}_S^{n-1} + \Delta t\,(\boldsymbol{\sigma}_S^n)', \tag{22}$$

where $(\boldsymbol{\sigma}_S^n)' := \lambda\,\mathrm{div}(\mathbf{v}_S^n)\,I + 2\,\mu\,\boldsymbol{\varepsilon}(\mathbf{v}_S^n)$ in Ω_S.

Let us define the bilinear forms $a : \mathbf{H}^1_0(\Omega)\times\mathbf{H}^1_0(\Omega) \to \mathbb{R}$ and $b : L^2(\Omega_F)\times\mathbf{H}^1_0(\Omega) \to \mathbb{R}$, and the linear functional $l^n \,:\, \mathbf{H}^1_0(\Omega) \to \mathbb{R}$:

$$\begin{aligned} a(\mathbf{v},\mathbf{w}) \;&:=\; \int_\Omega \rho\,\mathbf{v}\cdot\mathbf{w} \,+\, \int_\Omega \kappa\,\boldsymbol{\varepsilon}(\mathbf{v}) : \boldsymbol{\varepsilon}(\mathbf{w}) \,+\, \lambda\,(\Delta t)^2 \int_{\Omega_S} \mathrm{div}(\mathbf{v})\,\mathrm{div}(\mathbf{w})\,, \\ b(q,\mathbf{w}) \;&:=\; -\,\Delta t \int_{\Omega_F} q\,\mathrm{div}(\mathbf{w})\,, \quad \forall\, q \in L^2(\Omega_F), \\ l^n(\mathbf{w}) \;&:=\; \Delta t \int_\Omega \mathbf{f}(t_n)\cdot\mathbf{w} \,+\, \int_\Omega \rho\,\mathbf{v}^{n-1}\cdot\mathbf{w} \,-\, \Delta t \int_{\Omega_S} \boldsymbol{\sigma}_S^{n-1} : \boldsymbol{\varepsilon}(\mathbf{w})\,, \end{aligned} \tag{23}$$

for any $\mathbf{v}$, $\mathbf{w} \in \mathbf{H}^1_0(\Omega)$ and any $q \in L^2(\Omega_F)$. With these notations, problem (21) can be written as follows:
Given $\mathbf{v}^0$ and $\boldsymbol{\sigma}_S^0$, for $n = 1, 2, \ldots$, we look for $\mathbf{v}^n \in \mathbf{H}^1_0(\Omega)$, $p^n \in L^2(\Omega_F)$ such that

$$\left\{\begin{array}{rcll} a(\mathbf{v}^n,\mathbf{w}) \,+\, b(p^n,\mathbf{w}) \;&=\; l^n(\mathbf{w})\,, & \forall\,\mathbf{w} \in \mathbf{H}^1_0(\Omega)\,, \\ b(q,\mathbf{v}^n) \;&=\; 0\,, & \forall\, q \in L^2(\Omega_F)\,. \end{array}\right. \tag{24}$$

4.2 Finite element discretization

We consider now finite element subspaces $\mathbf{V}_h \subset \mathbf{H}^1_0(\Omega)$ and $Q_h \subset L^2(\Omega_F)$, such that $(\mathbf{V}_h|_{\Omega_F}, Q_h)$ is a stable pair for the Stokes problem. The corresponding fully discrete scheme to solve problem (1)–(3) reads as follows:

Given $\mathbf{v}^0$ and $\boldsymbol{\sigma}_S^0$, for $n = 1, 2, \ldots$, we look for $\mathbf{v}_h^n \in \mathbf{V}_h$, $p_h^n \in Q_h$ such that

$$\left\{ \begin{array}{rcll} a(\mathbf{v}_h^n, \mathbf{w}_h) + b(p_h^n, \mathbf{w}_h) & = & l^n(\mathbf{w}_h)\,, & \forall\, \mathbf{w}_h \in \mathbf{V}_h\,, \\ b(q_h, \mathbf{v}_h^n) & = & 0\,, & \forall\, q_h \in Q_h\,, \end{array} \right. \tag{25}$$

and then compute

$$\boldsymbol{\sigma}_S^n \,=\, \boldsymbol{\sigma}_S^{n-1} \,+\, \Delta t \left(\lambda \,\mathrm{div}(\mathbf{v}_h^n)\, I + 2\,\mu\, \boldsymbol{\varepsilon}(\mathbf{v}_h^n)\right).$$

5 NUMERICAL RESULTS

We implemented the fully discrete scheme (25) in a MATLAB code in the case $d = 2$, choosing the mini-element to approximate the solution in the fluid domain and piecewise linear elements in the solid domain.

In this section, we show some results for a particular test problem with the known solution

$$\begin{array}{rcl} v_1(t, \mathbf{x}) & = & \left\{ \begin{array}{ll} \cos x_2 \; e^t & \text{in } (0,1) \times \Omega_F, \\ (\cos x_2 + \sin x_1)\, e^t & \text{in } (0,1) \times \Omega_S, \end{array} \right. \\ v_2(t, \mathbf{x}) & = & \sin x_1 \; e^t \quad \text{in } (0,1) \times \Omega, \\ p(t, \mathbf{x}) & = & -2\, \cos x_1 \; e^t \quad \text{in } (0,1) \times \Omega_F, \end{array} \tag{26}$$

where $\Omega_F = (-1, 0) \times (-1, 1)$ and $\Omega_S = (0, 1) \times (-1, 1)$. We consider the case in which the fluid and the solid have similar mass densities; more precisely, we take $\rho_F = \rho_S = 1$. The kinematic viscosity is $\nu = \frac{1}{2}$ and the Lamé parameters are $\mu = \frac{1}{2}$ and $\lambda = 1$.

5.1 Validation of the spatial discretization

To start with, we test the choice of finite element spaces, that is, the mini-element in the fluid domain and piecewice linear elements in the solid domain. To this end, we solved the test problem for a fixed time. In particular, we took the time step $\Delta t = 1$ and used exact Dirichlet boundary conditions for the fixed time. We considered a sequence of meshes obtained by uniformly refining the initial mesh; we denote by $h = l, l/2, \ldots$ the corresponding mesh–sizes, N_h is the associated number of vertices and dof denotes the corresponding degrees of freedom (d.o.f.). The computed solutions, $\mathbf{v}_h = (v_{1,h}, v_{2,h})$, p_h, were compared with the exact one, $\mathbf{v} = (v_1, v_2)$, p, to determine the order of convergence.

In Table 1, we show the total number of vertices, the corresponding d.o.f., and the absolute errors for each unknown, that we denote $e_h(v_j) := ||v_j - v_{j,h}||_{H^1(\Omega)}$ $(j = 1, 2)$ and $e_h(p) := ||p - p_h||_{L^2(\Omega_F)}$. The corresponding experimental convergence rates for each unknown are shown in Table 2. The experimental convergence rate is computed for each pair of consecutive meshes as the slope in log-log scale of the error versus the number of vertices of the associated mesh:

$$r_h := -2\,\frac{\log e_{h/2} - \log e_h}{\log N_{h/2} - \log N_h}\,. \tag{27}$$

Table 1: Absolute errors for different meshes at a fixed time.

h	N_h	dof	$e_h(v_1)$	$e_h(v_2)$	$e_h(p)$
l	195	772	0.075514	0.043627	0.022462
$l/2$	737	3127	0.037705	0.021663	0.007871
$l/4$	2865	12595	0.018833	0.010744	0.002907
$l/8$	11297	50563	0.009400	0.005344	0.001071
$l/16$	44865	202627	0.004695	0.002666	0.000385

Table 2: Experimental convergence rates for successive meshes at a fixed time.

$r_h(v_1)$	1.044696	1.022568	1.012914	1.006846
$r_h(v_2)$	1.053087	1.032904	1.017875	1.008713
$r_h(p)$	1.577438	1.466830	1.455395	1.482009
$r_h(\mathbf{u}, p)$	1.070852	1.035734	1.020001	1.010696

We can observe that, as the mesh becomes finer, the experimental rate of convergence approaches 1 for both velocity components, whereas the method is superconvergent in the pressure variable, with rates of convergence that approach 1.5. It is important to remark that we have observed a similar behavior in other tests.

5.2 Validation of the time discretization

The main aim of this example is to study the stability of the numerical scheme (25) as the time step Δt becomes smaller. To this end, we chose the mesh of size $h = l/8$, and then decreased Δt as shown in Table 3. We remark that the associated errors, $e_h^{\Delta t}(v_j) := ||v_j - v_{j,h}^{\Delta t}||_{L^2((0,1),H^1(\Omega))}$ $(j = 1, 2)$ and $e_h^{\Delta t}(p) := ||p - p_h^{\Delta t}||_{L^2((0,1),L^2(\Omega_F))}$, stagnate faster for the velocity than for the pressure.

Table 3: Absolute errors for the mesh–size $l/8$ and different time steps.

Δt	$e_h^{\Delta t}(v_1)$	$e_h^{\Delta t}(v_2)$	$e_h^{\Delta t}(p)$
10^{-1}	0.039295	0.041494	0.238824
10^{-2}	0.017876	0.010804	0.023515
10^{-3}	0.018346	0.011303	0.003186
10^{-4}	0.022725	0.016331	0.002571

5.3 Numerical results for the fully discrete scheme

Finally, we present the numerical results obtained taking a fixed time step and successively refined meshes. In Tables 4 and 6 we show the results obtained for $\Delta t = 10^{-2}$ and $\Delta t = 10^{-3}$, respectively. The corresponding experimental convergence rates are shown in Tables 5 and 7.

Table 4: Absolute errors for successive meshes and the fixed time step $\Delta t = 10^{-2}$.

h	$e_h^{\Delta t}(v_1)$	$e_h^{\Delta t}(v_2)$	$e_h^{\Delta t}(p)$
l	0.152335	0.098009	0.053320
$l/2$	0.073220	0.045141	0.029586
$l/4$	0.035434	0.021105	0.024505
$l/8$	0.017876	0.010804	0.023515

Table 5: Experimental convergence rates for successive meshes and the fixed time step $\Delta t = 10^{-2}$.

$r_h(v_1)$	1.102011	1.069099	0.997426
$r_h(v_2)$	1.166158	1.119933	0.976049
$r_h(p)$	0.885995	0.277532	0.060108
$r_h(\mathbf{v}, p)$	1.098631	0.942423	0.615441

For $\Delta t = 10^{-2}$, the experimental convergence rates are around 1 for the two components of the velocity, but this time step appears to be too rough to obtain good convergence behavior in the pressure variable. This problem can be solved using a smaller Δt. Indeed, we can observe in Table 7 that for $\Delta t = 10^{-3}$ a good convergence behavior is obtained for the pressure too.

Acknowledgements. The research of the authors was partially supported by the MEC research project MTM2010-21135-C02-01.

Table 6: Absolute errors for successive meshes and the fixed time step $\Delta t = 10^{-3}$.

h	$e_h^{\Delta t}(v_1)$	$e_h^{\Delta t}(v_2)$	$e_h^{\Delta t}(p)$
l	0.194069	0.147480	0.054495
$l/2$	0.092336	0.067421	0.017108
$l/4$	0.040903	0.027274	0.006349
$l/8$	0.018346	0.011303	0.003186

Table 7: Experimental convergence rates for successive meshes and the fixed time step $\Delta t = 10^{-3}$.

$r_h(v_1)$	1.117301	1.199388	1.1687576
$r_h(v_2)$	1.177398	1.333136	1.284060
$r_h(p)$	1.742736	1.460054	1.005267
$r_h(\mathbf{v}, p)$	1.158779	1.247323	1.198638

REFERENCES

[1] S. Dasser, A penalization method for the homogenization of a mixed fluid–structure problem, *C.R. Acad. Sci. Paris Ser. I Math.* (1995) **320**:759–764.

[2] Q. Du, M.D. Gunzburger, L.S. Hou and J. Lee, Analysis of a linear fluid–structure interaction problem, *Discrete and Continuous Dynamical Systems* (2003) **9(3)**:633–650.

[3] Q. Du, M.D. Gunzburger, L.S. Hou and J. Lee, Semidiscrete finite element approximations of a linear fluid–structure interaction problem, *SIAM J. Numer. Anal.* (2004) **42**:1–29.

[4] D. Errate, M.J. Esteban and Y. Maday, Couplage fluide–structure: Un modéle simplifié en dimension 1, *C.R. Acad. Sci. Paris Sér. I Math.* (1994) **318**:275–281.

[5] C. Farhat, M. Lesoinne and P. LeTallec, Load and motion transfer algorithms for fluid/structure interaction problems with non–matching discrete interfaces: Momentum and energy conservation, optimal discretization and application to aeroelasticity, *Comput. Meth. Appl. Mech. Engrg.* (1998) **157**:95–114.

[6] O. Kayser–Herold and H.G. Matthies, A unified least–squares formulation for fluid–structure interaction problems, *Computers and Structures* (2007) **85**:998–1011.

[7] R. Schulkes, Interactions of an elastic solid with a viscous fluid: Eigenmode analysis, *J. Comput. Phys.* (1992) **100**:270–283.